3. A Brief Review of Thermodynamics, Part 1

J. S. Wright
jswright@tsinghua.edu.cn

3.1 Overview

This chapter reviews some of the key thermodynamics concepts and formulae needed for understanding the atmosphere–ocean system. Some relevant aspects of the first and second laws of thermodynamics are summarized, with applications to the atmosphere and ocean. The thermodynamics of the ocean are presented and discussed, including the sources and importance of density variations and vertical instability. An extension to the energy balance model framework is derived to illustrate the relevance of ocean thermodynamics to climate sensitivity.

3.2 Energy Conservation and the First Law

The first law of thermodynamics states that energy is conserved in an isolated system. Increasing the internal energy of a substance (such as a parcel of air or a volume of seawater) requires an equal reduction of energy elsewhere.

Energy transfer in the atmosphere and ocean may manifest as the expansion or contraction of a substance. Expansion requires the addition of energy to the substance, while contraction requires the removal of energy from the substance. As a substance expands, it does work by pushing against its environment. The amount of work done during expansion is equal to the environmental pressure times the change in volume (i.e., pdV). It is often useful to convert volume (an extensive property that depends on mass) to density (an intensive property that does not depend on mass):

$$\frac{dV}{m} = \frac{1}{\rho}. \tag{3.1}$$

The change in internal energy per unit mass can then be written as $pd(\rho^{-1})$, where ρ^{-1} is sometimes referred to as the specific volume (often denoted by the symbol α).

Energy transfer may also manifest as a change in the temperature of a substance. If the volume of the substance is held constant during the change in temperature, the amount of energy transferred is $c_v dT$ (where c_v is the specific heat at constant volume). The specific heat is defined as the amount of energy needed to warm a unit mass of the substance by a temperature 1 K, and can be defined with respect to either constant volume (c_v) or constant pressure (c_p). In the former case the pressure increases by the amount necessary to keep the volume constant, while in the latter case the volume expands by the amount necessary to keep the pressure constant.

The total amount of energy per unit mass that must be added to change both the temperature and volume of a substance is therefore

$$\delta Q = c_v dT + pd(\rho^{-1}) = c_p dT + \rho^{-1} dp \tag{3.2}$$

where Q is the internal energy of the substance. The first term on the right hand side represents the change in thermal energy, and the second term represents the work done on (or by) the substance. A system is considered to be in **thermodynamic equilibrium** when the internal energy is distributed randomly throughout the system.

3.3 Adiabatic Processes and the Second Law

An **adiabatic process** is any process that occurs without the addition or loss of internal energy (i.e., $\delta Q = 0$). Adiabatic processes may also be called isentropic processes, because the entropy is constant throughout the process (provided that the system remains close to thermodynamic equilibrium, which is the case for most processes in the atmosphere and ocean). For our purposes, entropy is defined so that its change ds is equal to $\delta Q/T$. In the atmosphere, we can use the equation of state (Eq. 2.1) to show that

$$ds \equiv \frac{\delta Q}{T} = c_p \frac{dT}{T} - R_d \frac{dp}{p} = c_p d\ln(T p^{-R_d/c_p}) \tag{3.3}$$

For a more complete derivation and discussion of entropy in the atmosphere–ocean system, see, e.g., *Curry and Webster* (1999).

The second law of thermodynamics states that entropy never decreases in an isolated system provided that energy is neither added nor removed. Stated another way, heat is only transferred from hotter parts of the system to colder parts of the system. Adiabatic processes (for which the change in entropy is zero) are reversible because the initial state of the system can be retrieved by reversing the process. By contrast, diabatic (non-adiabatic) processes are irreversible.

Consider for example an air parcel moved from a high altitude (where pressure is low) to a lower altitude (where pressure is high). Assume that the transfer is effectively instantaneous, so that the parcel has no opportunity to exchange heat with its surroundings. In this case, the entropy does not change. Accordingly,

$$ds = c_p d\ln(T p^{-R_d/c_p}) = 0 \tag{3.4}$$

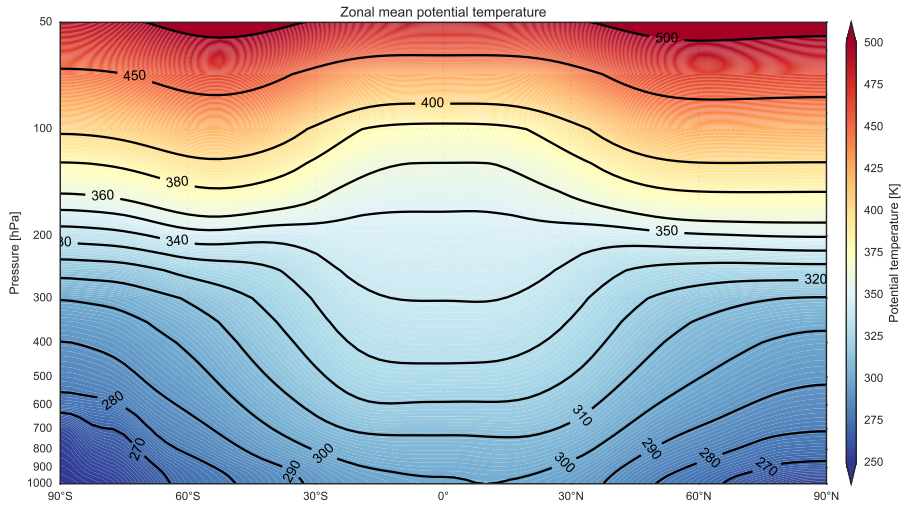

Figure 3.1: The distribution of potential temperature with pressure and latitude. Data from the Climate Forecast System Reanalysis.

so that the temperature T_0 arrived at by compressing a parcel at temperature T and pressure p to a pressure p_0 can be found by setting Tp^{-R_d/c_p} equal to $T_0 p_0^{-R_d/c_p}$. The **potential temperature** θ is defined as the temperature an air parcel would have if it were compressed adiabatically to a reference pressure p_0:

$$\theta = T\left(\frac{p}{p_0}\right)^{-R_d/c_p}. \tag{3.5}$$

The reference pressure p_0 is typically taken to be 1000 hPa for potential temperature in the atmosphere. Like entropy, potential temperature is conserved for adiabatic processes. Unlike temperature, potential temperature increases monotonically with height throughout the zonal mean atmosphere (Fig. 3.1). The vertical gradient of potential temperature is a good measure of stability in the atmosphere, as we will see in the next chapter. Decreases in potential temperature with height are eliminated very efficiently by convection.

Potential temperature can be similarly defined for the ocean to remove the effects of compressibility on the variation of temperature with depth. This is particularly important for the deep ocean, where extremely high pressures (up to 1000 atm) mean that compressibility has important effects on the vertical variation of temperature. For the ocean, potential temperature is calculated by theoretically raising an ocean parcel to a reference pressure from greater depths (where pressure is higher than the reference pressure). The reference pressure depends on the depth of the water mass, and is generally taken to be 1013 hPa (1 atm) for the upper ocean and 100 bar (~1 km), 200 bar (~2 km), or 400 bar (~4 km) for progressively deeper layers of the ocean.

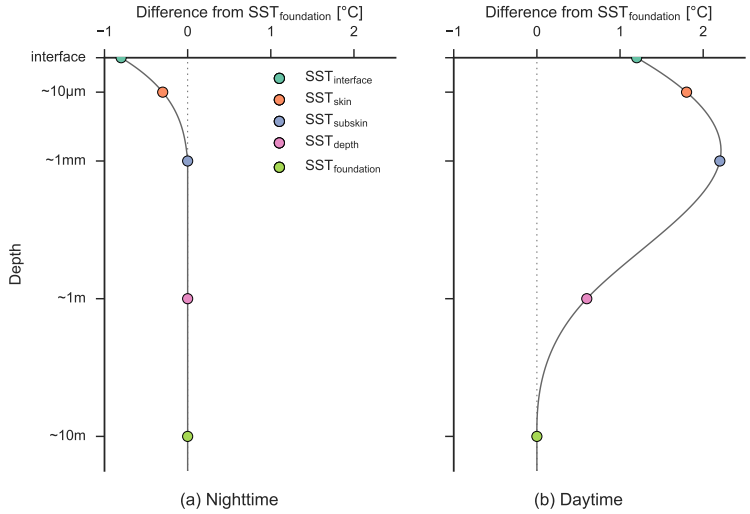

Figure 3.2: Schematic of idealized temperature deviations from mean sea surface temperature (a) at night and (b) during the day under calm conditions (after *Kawai and Wada*, 2007).

3.4 Thermodynamics of the Ocean

Chapter 1 introduced the structure and composition of the global ocean. Here, we examine the bulk thermodynamic properties of both the ocean as a whole and the water that makes it up, and then develop a simple but informative model of the climate system that applies these concepts.

3.4.1 Thermal inertia

One of the most important climatological properties of the ocean is its immense thermal inertia. The specific heat of liquid water is second largest among all liquids. The large specific heat of liquid water and the ability of water to quickly equalize internal variations in pressure mean that the temperature range within the global ocean is small (~ 30°C). Integrated over the entire ocean (which contains 1.4×10^{21} kg of seawater) this large specific heat becomes a large thermal inertia, which plays a key role in the long-term stability of climate.

The ocean responds slowly to variations in sunlight, with diurnal (daily) temperature variations of only 0.2–0.6°C on average (Fig. 3.2). The amplitude of the diurnal cycle in sea surface temperature depends on both latitude and season. The very top layers of the ocean may warm by 1–2°C on calm, sunny days, but this warming is generally limited to the top 1 m. Windy conditions can mix the warming to greater depths (up to 10 m or more), but reduce the magnitude of the daytime temperature increase (Fig. 3.3). Seasonal variations in temperature in the upper ocean are larger due to the longer duration of changes in incoming solar radiation at the surface, especially in the mid-latitudes (Fig. 3.4). Seasonal changes in insolation at high

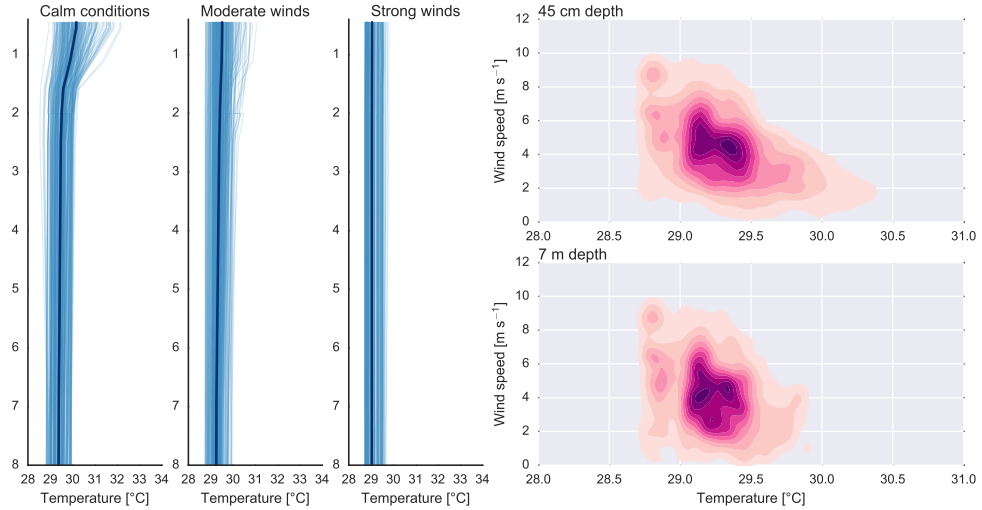

Figure 3.3: Vertical temperature profiles in the tropical western Pacific under different surface wind conditions (left) and joint distributions of surface wind and temperature at 45 cm (top right) and 7 m (bottom right) depth. Data from the TOGA COARE campaign, collected at 1° 45′S, 156°E between 21 October 1992 and 4 March 1993.

latitudes in the northern hemisphere have a dramatic impact on Arctic sea ice extent (Fig. 3.5).

The high specific heat of water is a consequence of the strength of hydrogen bonds. The strength of these bonds in the condensed phase also leads to water having an unusually large **latent heat of vaporization**, which is defined as the amount of energy required to convert 1 kg of liquid water to water vapor. Phase transitions (such as the evaporation of liquid water) are reversible: the amount of energy released when vapor condenses to liquid is equal to the amount of energy required to convert the same amount of liquid to vapor. Figure 3.2b indicates that the temperature at the atmosphere–ocean interface is cooler than the temperature at approximately 1 mm depth. This temperature distribution reflects the effect of evaporation and associated cooling at the ocean surface. The latent heat flux from the ocean to the atmosphere is a key component of the global energy budget (see also Fig. 1.13).

The presence of dissolved salts changes the thermodynamic properties of seawater. For example, the freezing point, specific heat, and latent heat of vaporization for seawater all decrease with increasing salinity. The freezing point of seawater with a salinity of 35 psu is approximately −2°C, and profiles of temperature with depth show that time mean temperatures in parts of the high latitude ocean can be colder than 0°C (Fig. 2.5). The specific heat at constant pressure decreases from approximately 4200 J kg^{-1} K^{-1} for pure water at 0°C to approximately 4000 J kg^{-1} K^{-1} for seawater with a salinity of 35 psu. Similarly, the latent heat of vaporization decreases from approximately 2.5×10^6 J kg^{-1} to approximately 2.4×10^6 J kg^{-1}. These changes indicate that the presence of dissolved salts weakens the hydrogen bonds in liquid water.

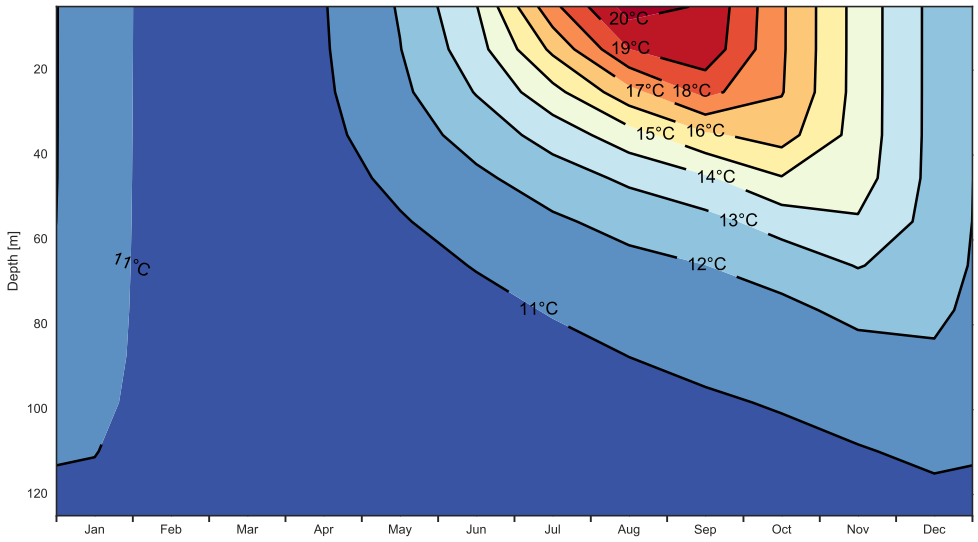

Figure 3.4: Seasonal cycle of potential temperature with depth in the North Pacific (180°E–200°E; 35°N–45°N). Data from the ORAS4 ocean reanalysis.

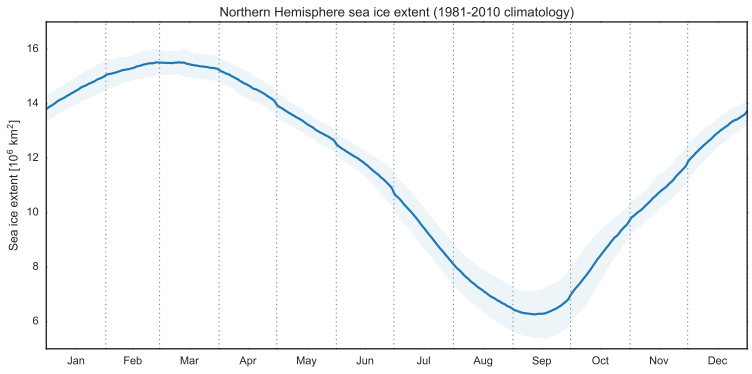

Figure 3.5: Climatological annual cycle of sea ice extent in the Arctic during 1981–2010. The uncertainty window shows one standard deviation around the mean. Data from the NSIDC Sea Ice Index.

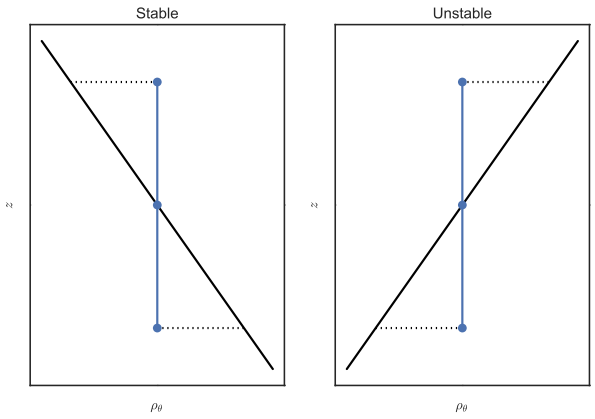

Figure 3.6: Stability of a parcel perturbed from equilibrium.

3.4.2 VERTICAL STABILITY

A fluid is said to be **stable** if a parcel displaced to a new vertical position tends to return to its original position, and **unstable** if the displaced parcel continues to rise or sink following displacement. Vertical stability therefore depends fundamentally on the vertical profile of density (Fig. 3.6). The force on a parcel that is denser than its surroundings will cause the parcel to accelerate downwards. Such a parcel is said to have negative buoyancy. Conversely, the **buoyancy force** is upward on a parcel that is less dense than its surroundings.

The magnitude of the buoyancy force per unit volume on a parcel displaced by a distance δz from its equilibrium density ρ_e can be calculated as the gravitational acceleration times the difference between the environmental density and ρ_e:

$$g\left[\rho_e + \left(\frac{\partial \rho}{\partial z}\right)\delta z - \rho_e\right] = g\left(\frac{\partial \rho}{\partial z}\right)\delta z \tag{3.6}$$

A parcel displaced adiabatically upward will therefore be positively buoyant if $\frac{\partial \rho}{\partial z} > 0$, neutrally buoyant if $\frac{\partial \rho}{\partial z} = 0$, and negatively buoyant if $\frac{\partial \rho}{\partial z} < 0$. These three conditions respectively correspond to a fluid that is unstable, neutrally stable, and stable.

Based on Eq. 3.6, it is clear that the acceleration due to the buoyancy force depends on both the magnitude of the vertical density gradient and the extent of the displacement:

$$\frac{d^2}{dt^2}\delta z = \left(\frac{g}{\rho_e}\frac{\partial \rho}{\partial z}\right)\delta z \tag{3.7}$$

This equation is similar to the simple harmonic oscillator equation

$$\frac{d^2 z}{dt^2} = -N^2 z,$$

for which the period of the oscillator is equal to $2\pi/N$. In this case,

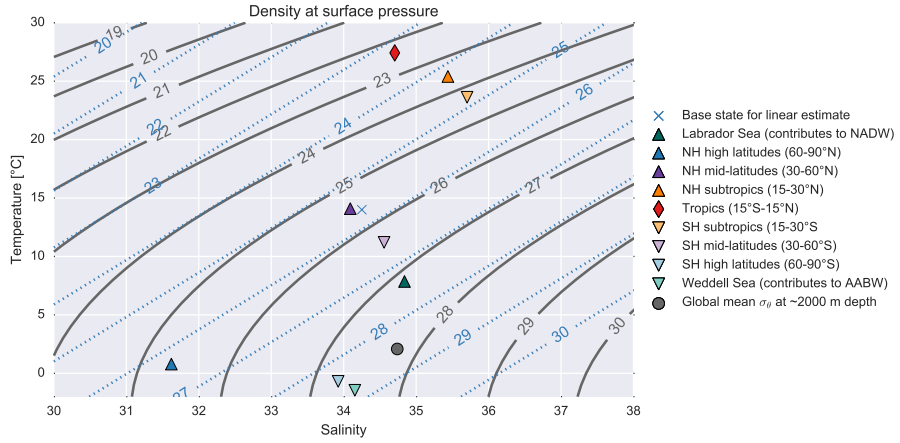

Figure 3.7: Density of seawater (σ) at atmospheric pressure as a function of temperature and salinity. Values calculated using the `gsw` module are shown as solid contours and values based on Eq. 3.10 are shown as dashed blue contours (the base state around which Eq. 3.10 is linearized is shown as a blue 'x'). Values of surface density in different latitude bands and ocean basins are shown for reference, along the global mean potential density at ~2000 m depth. Data from the ORAS4 ocean reanalysis.

$$N^2 = \left(-\frac{g}{\rho_e}\frac{\partial \rho}{\partial z}\right) \tag{3.8}$$

so that

$$N = \sqrt{\left(-\frac{g}{\rho_e}\frac{\partial \rho}{\partial z}\right)}. \tag{3.9}$$

Note that $\frac{g}{\rho_e} > 0$, so the density gradient must be negative upwards (stable) for oscillations to occur (i.e., for N to be real). Buoyancy oscillations (also called gravity waves) are ubiquitous in the atmosphere and ocean, and play a fundamental role in fluid dynamics. The frequency of a buoyancy oscillation depends on the magnitude of the density gradient, with a stronger density gradient corresponding to a faster oscillation. For example, gradients in the upper ocean thermocline are much larger than those in the deep ocean (Fig. 2.6). The frequency of internal gravity waves is therefore greater in the upper ocean (where the typical period is approximately 10 minutes) than in the deep ocean (where the typical period is closer to two days).

The above criteria for stability can be applied to the ocean, provided adiabatic effects are taken into account. As discussed in section 1.5.1, the density of seawater depends on pressure, temperature, and salinity. From the perspective of the ocean, where pressure increases rapidly with depth (Fig. 2.4), sea level pressure is roughly constant. Density variations in the surface ocean therefore depend mainly on variations in temperature and salinity. The variation of

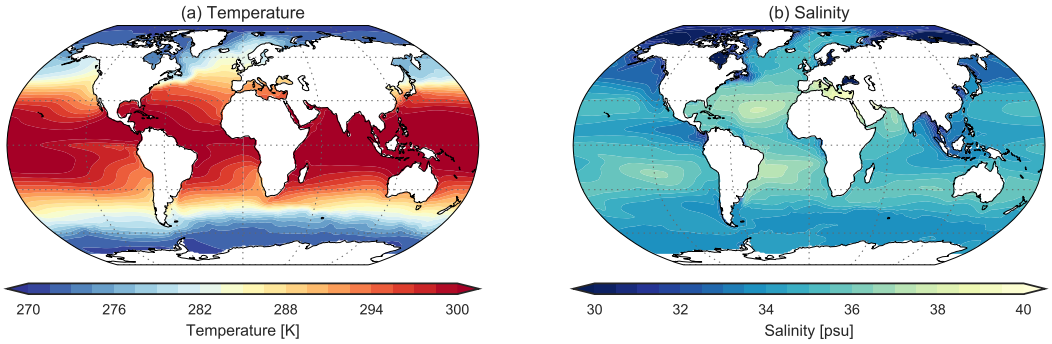

Figure 3.8: (a) Temperature and (b) salinity of seawater at ~5 m depth. Data from the ORAS4 ocean reanalysis.

density with temperature and salinity at atmospheric pressure is shown in Fig. 3.7. Two approximations are shown: a linearized estimate and an estimate based on the empirically-based formula implemented in the `gsw` python module. The linearized estimate is calculated using the formula:

$$\rho = \rho_0 \left(1 - \alpha(T - T_0) + \beta(S - S_0)\right) \tag{3.10}$$

with $\alpha = 2 \times 10^{-4}\,\mathrm{kg\,m^{-3}\,K^{-1}}$ and $\beta = 7.6 \times 10^{-4}\,\mathrm{kg\,m^{-3}\,psu^{-1}}$. This estimate is linearized around a reference state with $\rho_0 = 1025.65\,\mathrm{kg\,m^{-3}}$, $T_0 = 14°\mathrm{C}$ and $S_0 = 34.25\,\mathrm{psu}$, which is roughly equivalent to the state of surface waters in Northern Hemisphere mid-latitudes (Fig. 3.7). The estimates are fairly accurate for values of T and S near this reference state, but fail at values of T and S that are far from the reference state.

The values of density calculated using the `gsw` module are more sensitive to changes in salinity than to changes in temperature at lower temperatures. Furthermore, the curvature of isopycnals (lines of constant density) in temperature–salinity space means that mixing between two water masses with the same density will produce water that is denser than either of the two original water masses. Both of these properties of seawater play important roles in the formation of dense water near the surface at high latitudes, where horizontal gradients in temperature and salinity can be quite sharp (Fig. 3.8). Mixing across sharp gradients in temperature and salinity is particularly important in the North Atlantic (Labrador Sea), where eddies (vortices) associated with the North Atlantic Current mix warm, salty water from the Gulf Stream with cold, fresh water exiting the Arctic Ocean, and in the Southern Ocean, where eddies associated with the Antarctic Circumpolar Current have a similar impact. These mixing effects yield some of the densest surface waters on Earth (Fig. 3.7), namely North Atlantic Deep Water (NADW) and Antarctic Bottom Water (AABW). The formation of these dense water masses is critical for the maintenance of the global overturning ocean circulation, which is called the **thermohaline circulation** because it depends on density variations driven by changes in temperature ("thermo-") and salinity ("-haline"). We will discuss these ideas further in lecture 8.

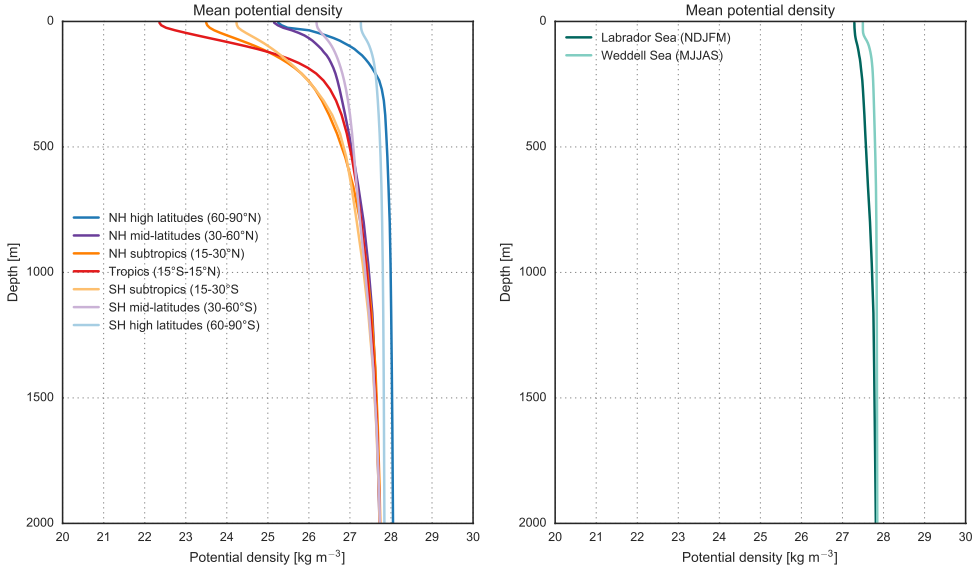

Figure 3.9: Annual mean profiles of potential density (σ_θ) in various latitude bands (left) and winter mean profiles of σ_θ in two ocean basins that contribute substantially to deep water formation (right). Data from the ORAS4 ocean reanalysis.

Section 3.3 introduced the concept of potential temperature, which is conserved during adiabatic motions. To analyze the vertical stability of the ocean, we introduce a similar concept, **potential density**. The potential density σ_θ of a volume of seawater is defined as the density that water would have if it were moved adiabatically to a reference level with no change in salinity. Just as with potential temperature, the reference level is typically defined to be sea level for the upper ocean, transitioning to depths of 1 km, 2 km, and 4 km for progressively deeper ocean layers (the choice of reference level also depends on the problem we want to address). The ocean is stable if potential density increases with increasing depth, neutrally stable if the vertical gradient of potential density is zero, and unstable if the potential density decreases with depth (i.e., denser water overlies water that is less dense). Figure 3.9 shows vertical profiles of potential density with depth for various latitudes. Like density, potential density is most effectively calculated using specially-designed software, such as the `gsw` module.

Unstable density gradients are removed efficiently and effectively by convective instability, which is the condition that results when the potential density gradient is positive upwards (i.e., N^2 is negative). Unstable density gradients are therefore observed only rarely. The presence of convective instability must be identified by looking instead for well-mixed ocean layers, where the potential density gradient is approximately neutral. Convective mixing in the ocean is most common during winter in high latitudes when strong surface cooling increases the density of surface water, possibly destabilizing the water column (right panel of Fig. 3.9). The depth of convection depends on the vertical profile of potential density. The strong stability of the upper ocean at most latitudes limits convective instability and associated overturning,

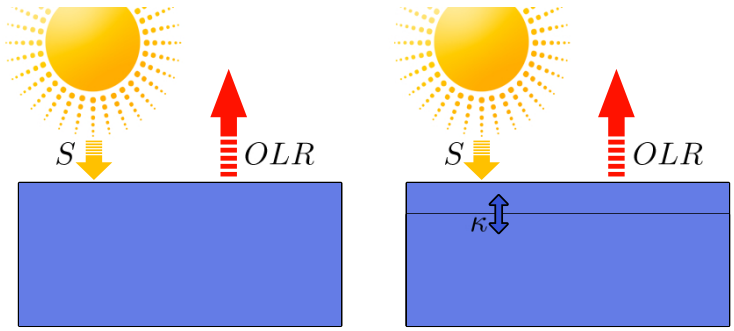

Figure 3.10: Schematic diagrams of (left) the one-box ocean climate model, and (right) the two-box ocean model.

effectively decoupling the surface mixed layer from the deep ocean. The climatic importance of this decoupling will become evident in the next section.

3.4.3 The two-box ocean energy balance model

Suppose we have a planet for which the surface is entirely covered by ocean. We can extend the energy balance models from chapter 1 to investigate the response timescale of this climate system to changes in the energy budget.

Let's initially assume that the ocean is entirely well-mixed. The total heat capacity of the ocean per unit area is then

$$\mu = \rho c_p D \tag{3.11}$$

where D is the depth of the ocean. The rate of temperature change at the surface of the ocean can be modeled as a function of the imbalance in the energy budget:

$$\mu \frac{dT_s}{dt} = S(\alpha) - OLR(T, \varepsilon) \tag{3.12}$$

where $S(\alpha) = (1-\alpha)Q$ is the incoming flux of solar radiation and $OLR(T,\varepsilon) = \varepsilon\sigma T_s^4$ is the outgoing flux of long-wave radiation (left panel of Fig. 3.10). As in Chapter 1, the parameter α represents the effective global albedo, the parameter Q the incoming flux of solar radiation at the top of the atmosphere, and the parameter ε represents the effects of greenhouse gases in the atmosphere (with a smaller value of ε corresponding to a stronger greenhouse effect). In the absence of an absorbing atmosphere, OLR depends only on T.

In equilibrium, $OLR(T_0,\varepsilon) = S(\alpha)$ and the rate of temperature change is zero. Assume some change in the composition of the atmosphere that decreases ε, thereby enhancing the greenhouse effect (emission of carbon dioxide by burning fossil fuels is one example). This change reduces OLR so that it is no longer equal to S. Examination of equation 3.12 indicates that this change in atmospheric composition forces an increase in surface temperature. Figure 3.11 shows the evolution of temperature following a reduction in ε from 0.615 to 0.6 for well-mixed

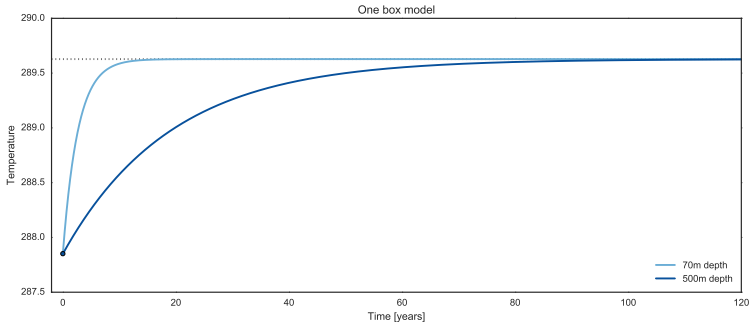

Figure 3.11: Adjustment of one-box oceans with depths of 70 m and 500 m to a change in ε from 0.615 to 0.6. The initial conditions are marked with a blue disc.

one-box 'oceans' 70 m and 500 m deep. The new equilibrium temperature, 289.63 K, is reached within a few years for the case with $D = 70$ m, but takes nearly 100 years for the case with $D = 500$ m.

We learned in Chapter 2 that the ocean is approximately 4000 m deep on average, and in Section 3.4.1 that only the uppermost part of the ocean responds to surface variations, with the deep ocean largely isolated. The deep ocean is not completely isolated from the surface, however, particularly at long timescales. A more appropriate energy balance model may therefore divide the ocean into two boxes rather than only one (right panel of Fig. 3.10), with temperature diffusion between the surface layer and the deep ocean:

$$\mu_m \frac{dT_m}{dt} = S(\alpha) - \kappa(T_m - T_o) - OLR(T, \varepsilon) \tag{3.13}$$

$$\mu_o \frac{dT_o}{dt} = \kappa(T_m - T_o) \tag{3.14}$$

where the subscripts m and o refer to the surface mixed layer and the deep ocean respectively and κ is the thermal diffusivity between the surface layer and the deep ocean. The deep ocean layer is generally assumed to be much thicker than the surface layer, so that $\mu_o \gg \mu_m$. Figure 3.12 shows the evolution of temperature in the surface mixed layer (assumed to be 70 m deep) and the deep ocean (4000 m deep) of a two-box ocean model with the same initial and boundary conditions as the one-box ocean model discussed above. This model takes thousands of years to equilibrate, as opposed to less than 10 years for the one-box model with a surface mixed layer 70 m deep and less than 100 years for the one-box model with a surface mixed layer 500 m deep (Fig. 3.11). It is important to remember that diffusion is not the main process governing heat exchange between the surface mixed layer and deep ocean in the real world, which instead depends on the situational deep convection discussed in the previous section.

An alternative, and perhaps more useful, formulation of this energy balance model can be achieved by calculating the new equilibrium temperature and then simulating the decay of the imbalance. The equilibrium temperature

$$T_{eq} = \sqrt[4]{\frac{(1-\alpha)Q}{\varepsilon\sigma}}$$

can alternatively be expressed as $T_{eq} = T(t) - T'$, with T' the magnitude of the temperature disequilibrium. Here, T_{eq} is the new equilibrium temperature, after adjustment, different from the initial equilibrium temperature T_0. Assuming that T' is small, we can then take the first two terms of the Taylor series around T_{eq} to get Eq. 3.12 in terms of T' (which approaches zero as the system approaches equilibrium) rather than T (which approaches T_{eq} as the system approaches equilibrium):

$$\mu\frac{dT'}{dt} = -\beta T' \tag{3.15}$$

where the parameter β is the derivative of $OLR(T)$ with respect to T at T_{eq}. Note that if albedo is also a function of T, then $\beta = \alpha'(T_{eq}) + OLR'(T_{eq})$. In the absence of feedbacks, $\beta \approx 4\varepsilon\sigma T^3$ for the black body approximation to OLR and $\beta = B \approx 2.09\,\mathrm{W\,m^{-2}\,K^{-1}}$ for Budyko's empirical approximation to OLR (Eq. 1.10). Positive feedbacks decrease the ability of the climate system to eliminate imbalances, and therefore reduce the magnitude of β. Negative feedbacks increase the ability of the climate system to eliminate imbalances, and therefore increase the magnitude of β.

The initial value $T'_0 = T_0 - T_{eq}$ can be approximated as

$$T'_0 = -\frac{\Delta F}{\beta}, \tag{3.16}$$

where $\Delta F = S(\alpha) - OLR(T_0)$. The value T'_0 is often referred to as the **equilibrium climate sensitivity** to the forcing ΔF. This response is independent of the heat capacity of the ocean. However, the timescale to reach T_{eq} does depend on the heat capacity. Eq. 3.15 has the analytical solution

$$T'(t) = T'_0 \exp\left(-t/\tau\right) \tag{3.17}$$

where $\tau = \mu/\beta$ is the adjustment timescale of the climate system (i.e., the ocean).

Note that none of these models consider the thermal adjustment of the atmosphere. This approximation is valid because long-wave cooling in the atmosphere eliminates temperature perturbations very quickly (see derivation of the atmospheric radiative relaxation timescale in Section 1.3.4). The two-box model can likewise be expressed in this modified framework as

$$\mu_m\frac{dT'_m}{dt} = -\beta T'_m - \kappa(T'_m - T'_o) \tag{3.18}$$

$$\mu_o\frac{dT'_o}{dt} = \kappa(T'_m - T'_o) \tag{3.19}$$

We should once more emphasize that, in reality, heat uptake by the deep ocean relies mainly on convective mixing (rather than diffusion). However, despite its simplicity, this simple two-box model can be used to derive powerful insights into the behavior of both the real climate

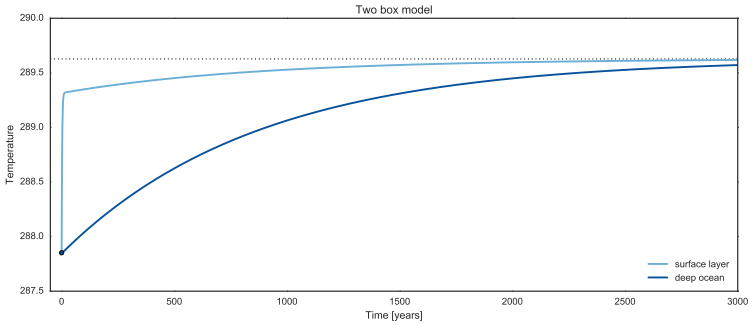

Figure 3.12: Adjustment of a two-box ocean model with a surface layer 50 m deep and a deep ocean 4000 m deep to a change in ε from 0.615 to 0.6. The initial condition is marked with a blue disc.

system and much more complicated global climate models (see, e.g., *Held et al.*, 2010, and references therein). The model parameters can also be modified to simulate other interactions between the coupled atmosphere–ocean system, such as the uptake or release of carbon dioxide by the ocean.

REFERENCES

Curry, J. A., and P. J. Webster (1999), *Thermodynamics of Atmospheres and Oceans*, 471 pp., Academic Press, London, U.K.

Held, I. M., et al. (2010), Probing the fast and slow components of global warming by returning abruptly to preindustrial forcing, *J. Climate*, *23*, 2418–2427.

Kawai, Y., and A. Wada (2007), Diurnal sea surface temperature variation and its impact on the atmosphere and ocean: A review, *J. Oceanogr.*, *63*, 721–744.